ARTICLES

AQCH ANALYTICAL AND QUANTITATIVE CYTOLOGY AND HISTOLOGY®

An Official Periodical of **The International Academy of Cytology** *and the* **Italian Society of Urologic Pathology**

Computer-Based Association of the Texture of Expressed Estrogen Receptor Nuclei with Histologic Grade Using Immunohistochemically-Stained Breast Carcinomas

Spiros Kostopoulos, M.Sc., **Dimitris Glotsos,** Ph.D., **Dionisis Cavouras,** Ph.D., **Antonis Daskalakis,** M.Sc., **Ioannis Kalatzis,** Ph.D., **Pantelis Georgiadis,** M.Sc., **Panagiotis Bougioukos,** M.Sc., **Panagiota Ravazoula,** M.D., and **George Nikiforidis,** Ph.D.

OBJECTIVE: To investigate the potential correlation between estrogen receptor (ER) texture and histologic grade in breast carcinomas.

STUDY DESIGN: Clinical material comprised 96 biopsies of infiltrative ductal carcinomas that were hematoxylin-eosin (H-E) and immunohistochemically (IHC) stained. H-E–stained specimens were used for tumor grading, and IHC-stained specimens were analyzed for ER-status estimation. Spearman's correlation test was used to estimate the relation between histologic grade and both the physician's ER-status assessment and a computer system's ER-status evaluation. Moreover, a pattern recognition system was developed that takes as input textural features extracted from ER-expressed nu-

From Medical Image Processing and Analysis Group, Laboratory of Medical Physics, School of Medicine, University of Patras; Department of Pathology, University Hospital of Patras, Rio; and Department of Medical Instruments Technology, Technological Educational Institute of Athens, Athens, Greece.

Messrs. Kostopoulos, Daskalakis, Georgiadis and Bougioukos are Ph.D. Candidates, Medical Image Processing and Analysis Group, Laboratory of Medical Physics, School of Medicine, University of Patras.

Drs. Glotsos and Kalatzis are Postdoctoral Researchers, Department of Medical Instruments Technology, Technological Educational Institute of Athens.

Dr. Cavouras is Professor, Department of Medical Instruments Technology, Technological Educational Institute of Athens.

Dr. Ravazoula is Medical Doctor, Department of Pathology, University Hospital of Patras.

Dr. Nikiforidis is Professor, Medical Image Processing and Analysis Group, Laboratory of Medical Physics, School of Medicine, University of Patras.

Address correspondence to: Spiros Kostopoulos, M.Sc., Laboratory of Medical Physics, School of Medicine, University of Patras, 26504 Rio, Greece (skostopoulos@upatras.gr).

Financial Disclosure: The authors have no connection to any companies or products mentioned in this article.

0884-6812/09/3104-0187/$18.00/0

clei and outputs the grade of the tumor. The system was evaluated using an external cross-validation procedure in order to assess its generalization to new cases.
RESULTS: Spearman's correlation revealed that the histologic grading was inversely related to both the physician's ER-status assessment and to the computer system's ER-status evaluation. The pattern recognition system was able to predict histologic grade with 95.2% accuracy. Important textural nuclear features were proven—the skewness, the angular second moment and the sum of entropy.
CONCLUSION: ER-expressed nuclei texture was found to contain important information related to histologic grade. (Anal Quant Cytol Histol 2009;31:187–196)

Keywords: cancer, breast; estrogen receptors; histologic grade; pattern recognition.

Studies concerning global cancer statistics indicate that breast cancer is the most frequent type of cancer among women.[1] To help with the diagnosis of breast cancer, many biologic factors have been proposed for their prognostic and predictive value. Among these factors, histologic tumor grade and estrogen receptor (ER) status have been noted for their importance and usefulness in clinical patient management.[2] Histologic grading is carried out based on the evaluation of visible features (such as grandular differentiation, nuclear pleomorphism, and mitotic count) on hematoxylin-eosin (H-E)–stained specimens.[3] ER status is estimated as a percentage of expressed nuclei on immunohistochemically (IHC)-stained specimens.[4]

Recent studies have attempted to discover possible links between H-E–stained and IHC-stained specimens—that is, examine whether histologic tumor grade relates to ER status.[5-9] Such a relationship seems to be important in the various treatment strategies followed with breast tumors.[6] To this end, preliminary findings have suggested that there might be a potentially meaningful inverse correlation between breast tumor grade and ER status. Accordingly, Desai et al[5] have reported a decrement in ER status when the tumors are poorly differentiated. Zafrani et al[6] have found a strong correlation between ER status and histologic grade ($p < 10^{-4}$). Fuqua et al[7] and Vagunda et al[8] have shown that histologic grade is inversely associated with ER status ($r_s = -0.40$, $p < 0.001$ and $r_s = 0.37$, $p = 0.036$, respectively). Baqai and Shousha[9] have also reported similar findings while working with ductal carcinomas in situ.

These conclusions imply that higher grade tumors are more likely to respond poorly to antiestrogens compared with lower grade tumors.[6] However, the quantification of ER status presents certain weaknesses. First, there is a lack of consensus among experts regarding the protocol to be followed for calculating the ER status. In some studies the American Society of Clinical Oncology recommendations are adopted,[4] suggesting that ER status should be the percentage of positively stained nuclei. Other clinical groups also take under consideration the nuclei staining intensity.[10] Second, an exact estimate of the ER status is difficult to obtain, because that would require manually counting positively expressed nuclei. In clinical practice a gross estimate often is obtained by histopathologists through visual inspection of representative specimen areas. Thus the evaluation of ER status, which has been considered by previous studies as the key measure for assessing the correlation between ERs and tumor grade, is prone to the physician's subjective estimation. Therefore more reliable methods are needed.

One alternative is to estimate the ER status in a more objective manner. Such a method has been presented by our group elsewhere.[11] Consequently, we have used this method to confirm the correlation of ER status and histologic grade. Another interesting alternative is to focus directly on the inherent properties of ERs inside the nuclei—namely, to look directly into the texture of expressed ER nuclei. The motivation for such an attempt has been inspired by the established connection of ER arrangement and distribution (i.e., texture) to chromatin alterations.[12-15] Taking into account that chromatin alterations reflect the grade of breast tumors,[16-21] directly associating the texture of expressed ER nuclei with tumor grade could be useful. Following this line of reasoning, a pattern recognition system was developed to automatically predict breast tumor grade based on textural features extracted from the nuclei of IHC-stained images. To the best of our knowledge, this has never been previously studied. The proposed system utilizes a probabilistic neural network classifier and was evaluated using an external cross-validation procedure in order to assess its generalization to new cases.

Material and Methods

Clinical Material and Evaluation

Archival material from 109 breast cancer cases of

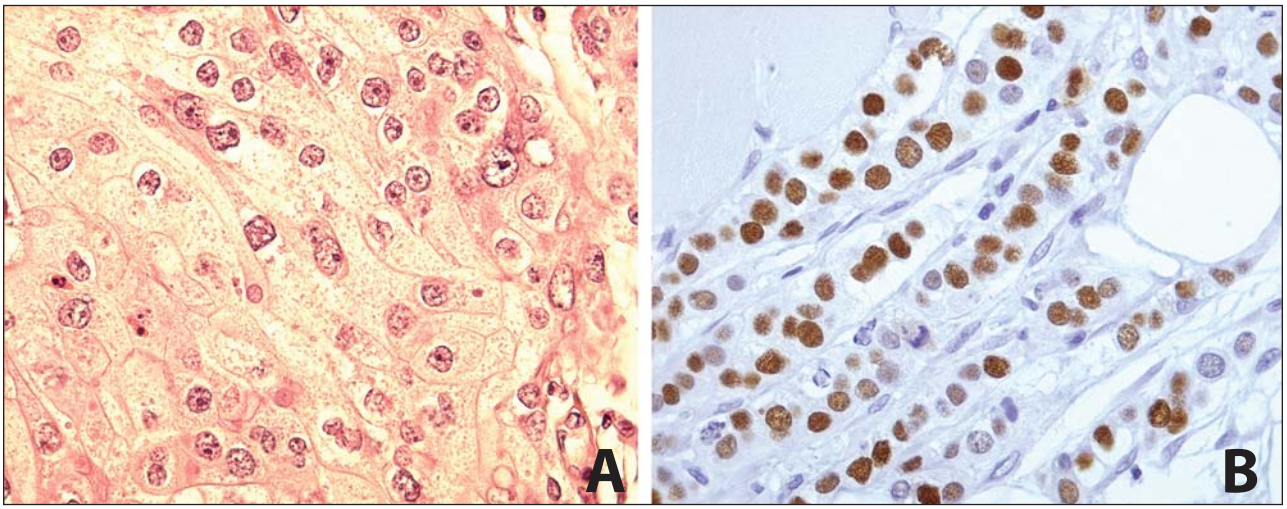

Figure 1 (A) Digitized frame from an H-E–stained specimen. (B) Digitized frame from an IHC specimen.

women who had undergone biopsy between 2000 and 2007 were collected from the Department of Pathology, University Hospital of Patras, Rio, Greece. All tumors were infiltrative (invasive) ductal carcinomas. For each case, H-E–stained and IHC-stained specimen tissues (Figure 1A and B, respectively) were generated from formalin-fixed, paraffin-embedded biopsy section tissues.

ER expression was assessed on IHC-stained specimens, following the clinical routine protocol[4] that takes into consideration the percentage ratio of ER-expressed nuclei (brown colored) to the total number of expressed and nonexpressed (blue) nuclei. Five percent was used as the cut-off value of ER expression for characterizing the case as having positive ER status. IHC evaluation was performed by the histopathologist without taking into consideration the corresponding histologic grade.

Tumor grade clinical assessment was carried out by a histopathologist (P.R.) on H-E–stained specimens following the World Health Organization recommendations and employing the Elston and Ellis grading scheme.[3] One month after initial assessment, the slides were resubmitted to the same histopathologist for a second reading. In cases with intraobserver variation, the physician and another histopathologist reviewed the slides on a multiheaded microscope (Olympus BX41; Olympus, Tokyo, Japan) in order to reach a consensus concerning tumor grade. Thirteen cases were omitted, 10 because their ER-stained slides could not be retrieved from the archive and 3 because of muddy or uneven staining. Thus a total of 96 cases were used for further processing.

Computer-Assisted Evaluation

For each of the cases, 5 nonoverlapping images ($1300\times1030\times36$ bit) were selected within regions on which the histopathologist's clinical assessment was based (Figure 1B). Selected images were acquired at a magnification of $\times400$ using a Zeiss Axiostar-Plus light microscope (Zeiss, Göttingen, Germany) and a Leica DC 300F color video camera (Leica, Wetzlar, Germany). Each digitized image was stored in an uncompressed tagged image format file (TIFF).

A schematic representation of this study is presented in Figure 2. The first goal was to confirm whether ER status correlated with histologic grade. To do this, we examined how strong the correlation of the visually estimated ER status was with respect to the histologic grade assigned from H-E–stained specimens. To confirm this correlation in more objective manner, a computer-based method was implemented that automatically quantified the ER status on IHC-stained images. Accordingly, a clustering algorithm was used to segment nuclei from surrounding tissue, and a supervised classification algorithm was employed to discriminate nuclei either as ER nonexpressed (Figure 3A) or ER expressed (Figure 3B). The latter method has been described in detail by our group elsewhere.[11] Correlation for both cases was computed using the Spearman's correlation coefficient.[22]

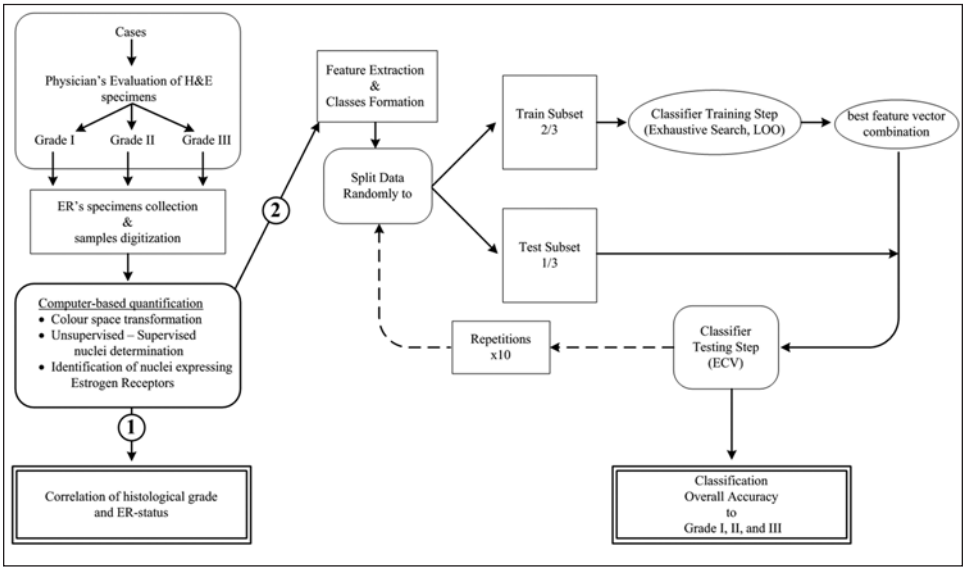

Figure 2 Block diagram of the study flowchart; (1) correlation of histologic grade with ER status and (2) classifier design and pattern recognition system evaluation for ERs texture relation with histologic grade. Schematic representation of system design.

Classification Into Grades

A pattern recognition system (PR system) was designed in order to classify breast cancer cases to malignant categories of grade I (low), grade II (intermediate) and grade III (high), using information from textural features extracted from only the ER-expressed nuclei. The design of the PR system consisted of 2 stages, a feature extraction and a system design and evaluation (classifier design and PR system evaluation).

Feature Extraction. Features expressing the distribution and arrangement of ERs in nuclei were calculated for each ER-expressed nucleus. Accordingly, each nucleus was represented by a 16-dimensional feature vector; 4 features (mean value, SD, skewness and kurtosis) were calculated from the 3-dimensional (3-D) nucleus's histogram (corresponding to red-green-blue [RGB] channels) and 12 features[23] (angular second moment, contrast, correlation, autocorrelation, sum of squares, inverse difference

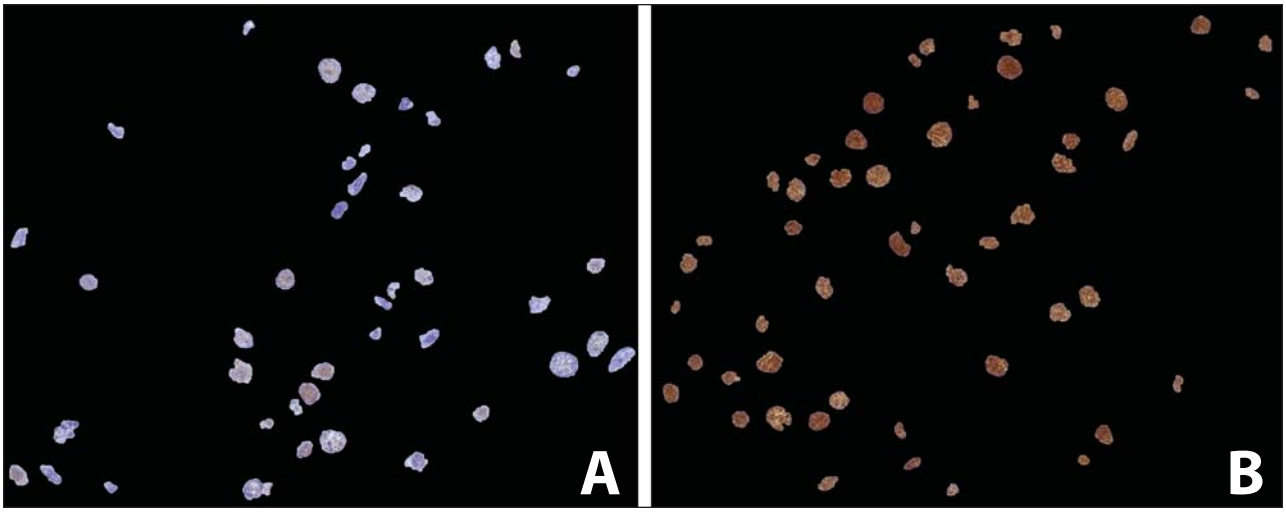

Figure 3 (A) ER-nonexpressed nuclei. (B) ER-expressed nuclei.

moment, entropy, sum of entropy, sum average, sum variance, difference variance and difference entropy) from the 3-D co-occurrence matrix.[24] Finally, each case was represented by a 16-dimensional feature vector, in which each feature was the average of the case's ER-expressed nuclei, picked from the case's 5 selected images.

2-Dimensional Co-Occurrence Matrix. When considering a grayscale image $I(x, y)$, the co-occurrence matrix[23] encoded the frequency of appearance of all possible gray-value pixel pairs in a particular orientation vector $\vec{D}$, with $\vec{D} = (d, \theta) \int (\Delta x, \Delta y)$, where d was the interpixel distance, $\theta \in \{0°, 45°, 90°, 135°, 180°, 225°, 315°\}$ and $(\Delta x, \Delta y)$ was the point displacement in the Cartesian space. According to Mahmoud-Ghoneim et al,[24] the joint probability function for each pixel pair in the co-occurrence matrix was calculated as:

$$P_{\vec{D}}(n,n') = \frac{1}{R}\sum_{x=1}^{K-\Delta x}\sum_{y=1}^{L-\Delta y}\delta(n,n') \quad (1)$$

$$\text{where } \delta(n,n') = \begin{cases} 1, \exists\, n,n' : I(\vec{c}) = n \wedge I(\vec{c}') = n' \\ 0, \text{otherwise} \end{cases},$$

where $\vec{c} = (x, y)$, $\vec{c}' = \vec{c} + \vec{D} = (x + \Delta x, y + \Delta y)$ with $x = 1,2,\ldots K$, $y = 1,2,\ldots L$ and K, L were the image dimensions, (n,n') were the gray values of the quantized image and R is the total number of possible neighboring pixel pairs. Thus R depends both on the image dimensions and on the orientation vector $\vec{D}$, according to $R = (K - \Delta x)(L - \Delta y)$. Therefore the 2-dimensional (2-D) co-occurrence matrix may be expressed as:

$$CM_{\vec{D}}(n+1, n'+1) = P_{\vec{D}}(n,n') \quad (2)$$

3-Dimensional Co-Occurrence Matrix. Palm[25] extended the concept of the classical co-occurrence matrices to the multichannel co-occurrence matrices that encode the frequency of appearance of all possible pixel pairs in different channels or bands. Assuming that a color image with 3 channels (i.e., RGB or Lab) could be seen as a 3-D image and could be expressed as a function of $f(\vec{m}) = f(x,y,z)$, the joint probability function for each pixel pair is given by:

$$P_{\vec{D}}(n,n') = \frac{1}{R}\sum_{x=1}^{K-\Delta x}\sum_{y=1}^{L-\Delta y}\sum_{z=1}^{M-\Delta z}\delta(n,n') \quad (3)$$

$$\text{where } \delta(n,n') = \begin{cases} 1, \exists\, n,n' : I(\vec{c}) = n \wedge f(\vec{m}) = n' \\ 0, \text{otherwise} \end{cases},$$

where $\vec{D} = (d,\theta,d_z) \int (\Delta x,\Delta y,\Delta z)$ is the orientation vector representing the point displacement in the 3-D axis and $R = (K-\Delta x)(L-\Delta y)(M-\Delta z)$. Similarly to equation 2, we have:

$$CM_{\vec{D}}(n+1, n'+1) = P_{\vec{D}}(n,n') \quad (4)$$

Thus, the 3-D co-occurrence matrix could be expressed as:

$$CM_{3D} = CM_{\vec{D}} + CM_{\vec{D}} \quad (5)$$

However, it has to be clarified that the 3 dimensions refer to the 3 channels of the color image (i.e., RGB or Lab)[25] and not to 3-D textural features extracted from volumetric regions of interest.

System Design and Evaluation. To assess the performance of the proposed method and provide a nearly unbiased estimate of the prediction error rate, the external cross-validation (ECV) method was used.[26,27] Accordingly, the ER-expressed dataset was randomly separated 10 times into 2 subsets: a training subset (70% of the data) and a testing subset (30% of the data). Each time, the training subset was used for designing the classifier and the test subset was used for assessing its predictive performance on new ER-expressed data.

Classifier Design. Classification was performed by means of the probabilistic neural network (PNN) classifier.[28] The PNN is implemented by a 4-layer (input, pattern, summation and output layers), feed-forward and 1-pass structure and encapsulates the Bayes' decision rule together with the Parzen estimators of the data's probability distribution function. The discriminant function of the PNN for class k was:

$$D_k(\mathbf{x}) = \frac{1}{(2\pi)^{d/2}\,\sigma^d}\,\frac{1}{N_k}\sum_{i=1}^{N_k}\exp\left[-\frac{(\mathbf{x}-\mathbf{x}_{ki})^T(\mathbf{x}-\mathbf{x}_{ki})}{2\sigma^2}\right] \quad (6)$$

where σ is the spread of the Gaussian activation function that was experimentally selected. The optimum value of the adjustable parameter σ of the Gaussian activation function was determined to be 0.24. N_k is the number of pattern vectors of class k, d is the dimensionality of pattern vectors and x_{ki} is the *i-th* pattern vector of class k. The unknown pattern vector, x, is classified to the class with the highest discriminant function value. An exhaustive search feature selection procedure was employed to determine the feature vector with the highest discriminatory accuracy. Accordingly, each feature vector

Table I *Histopathologist's Assessment of ER Status and Histologic Grading*

Grade	Cases	ER+	ER–
I	28	24	4
II	29	27	2
III	39	25	14
Total	96	76	20

combination was used to design the PNN classifier utilizing the leave-1-out method.[29]

For comparative purposes, the nearest neighbor,[29] the support vector machine (SVM)[30] and the logistic regression[31] classifiers were used. Additionally, the performance of the system using alternatively 2-D or 3-D co-occurrence matrix features was investigated. Finally, apart from RGB, the Lab color space[32,33] was used again for comparative purposes.

Results

Table I shows the distribution of cases according to their grading and the ER-positive and ER-negative status, as evaluated by the histopathologist. As can be seen from Table I, 79.2% (76 of 96) of the cases had an ER+ rate (expressed). While low grade cases (grade I) had a high ER+ rate (86%, 24 of 28), high-grade cases (grade III) had a lower ER+ rate (64%, 25 of 39), which is in agreement with the findings of previous studies.[5-9] Moreover, the majority of ER– (70%, 14 of 20) corresponded to the high grade cases.

Spearman's correlation revealed that the histologic grading was inversely related to both the physician's ER-status assessment ($r_s = -0.39$, $p < 0.001$) and to the computer system's ER-status evaluation ($r_s = -0.43$, $p < 0.001$). The attribute of diminishing ER status with increasing histologic grading might be also observed from Figure 4; the median of the ER status ranged from ~80% for low-grade cases to ~30% for high-grade cases. Also, as shown in the box plots of Figure 4, the variance increased with increasing histologic grading.

The classification performances of the PNN classifier employing the extracted ER-textural features over the course of 10 repetitions for the ECV procedure for the RGB and Lab color space are detailed in Tables II and III, respectively. The last column in Tables II and III, which contain the best feature vector combination at each repetition, demonstrate that the best feature vector combination size varied between 2 to 4 features. Moreover, the overall assessment of the accuracy to new data, as it might be obtained from the classification results employing the ECV, was 92.8%, with grade I scoring at 95%, grade II at 95.56% and grade III at 87.5% for the RGB color space. The Lab color space classification results were 95.2%, with grade I at scoring 95%, grade II at 98.89% and grade III at 91.25%.

An attempt to construct an operational PR system for assessing histologic grading through the 3 most frequently appearing features (skewness, angular second moment and sum of entropy) and the PNN classifier is shown in Figure 5, which is a scatter diagram with the 3 grading classes appearing well separated. The overall accuracy in discriminating among low, intermediate and high grades ranged from ~92–98%, with the mean value at 96.8%.

Table IV illustrates the comparative results under different color spaces, using either 2-D or 3-D co-occurrence–based features and different classification algorithms.

Discussion

Significant research studies[34,35] have been conducted in the search for more accurate methods of improving cancer diagnosis, treatment and prognosis. These studies have demonstrated the usefulness of nuclear features related to texture, morphology and shape,[16,20,36] using either commercial[37,38] or research software packages.[36,39,40]

The aim of this investigation was to quantitatively assess the correlation between ER status and histologic grade in an objective manner. Recent studies[5-9] have shown that a strong correlation exists between ER status and histologic grade and that

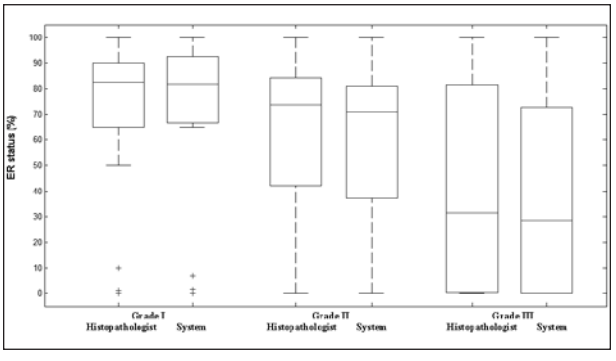

Figure 4 Boxplots of ER status and histologic grading. For each grade 2 box plots are illustrated, 1 corresponding to ER status visually estimated by the histopathologist and the other to ER-status automatically assessed by a computer-based system.

Table II *The PR-System's Classification Accuracy for 10 Repetitions of the ECV and the Corresponding Best Feature Combinations Under the RGB Color Space*

	Accuracy (%)				
ECV repetition	**Overall**	**Grade I**	**Grade II**	**Grade III**	**Feature vector**
1	92	100	100	75	skew, asm, ssq, idm
2	96	100	100	87.5	SD, skew, sentr
3	92	87.5	100	87.5	mv, krt, con
4	92	87.5	100	87.5	skew, asm, svar
5	96	100	100	87.5	skew, asm, sentr
6	100	100	100	100	SD, skew, sentr
7	88	100	88.9	75	mv, con, corr
8	96	87.5	100	100	SD, skew, sentr
9	84	100	66.7	87.5	asm, svar
10	92	87.5	100	87.5	skew, sentr
Average	92.80	95.00	95.56	87.50	
SD	4.54	6.45	10.73	8.33	

asm = Angular second moment, con = contrast, corr = correlation, idm = inverse difference moment, krt = kurtosis, mv = mean value, sentr = sum of entropy, skew = skewness, ssq = sum of squares, svar = sum variance.

this correlation is important in the various treatment strategies for breast tumors. These studies have lead us to investigate this correlation. The first goal of this study was to confirm that the ER status, as it is visually estimated by the histopathologist, is correlated with histologic tumor grade. Our results are in line with those presented in the literature,[5-9] indicating that a correlation does exists ($r_s = -0.39$, $p < 0.001$) and that the ER status is inversely related to tumors grade. To confirm this correlation in a more objective manner, we built a computer-based system[4,10] that automatically assessed the ER status on IHC-stained images, and we found an even stronger inverse correlation ($r_s = -0.43$, $p < 0.001$). However, because ER status may vary significantly from expert to expert and is strongly affected by both staining variations and the expert's experience,[12-15] this might not be the most reliable measure for studying such a correlation.

Thus we focused directly on the texture of expressed ER nuclei, which has been shown to vary with chromatin alterations.[12-15] To investigate the hidden biologic information imprinted as texture on ER-expressed nuclei, a PR system was developed that takes as input textural features and outputs the grade of the tumor. The overall accuracy of the system was 95.2%.

The PR system revealed 2 important conclusions.

Table III *The PR System's Classification Accuracy for 10 Repetitions of the ECV and the Corresponding Best Feature Combinations Under the Lab Color Space*

	Accuracy (%)				
ECV repetition	**Overall**	**Grade I**	**Grade II**	**Grade III**	**Feature vector**
1	96	87.5	100	100	SD, skew, asm
2	92	87.5	100	87.5	SD, asm, con
3	100	100	100	100	skew, krt, asm, con
4	96	100	100	87.5	mv, SD, sentr
5	96	100	100	87.5	krt, con
6	100	100	100	100	skew, corr, idm
7	88	75	100	87.5	SD, corr, svar
8	96	100	100	87.5	skew, asm, sentr
9	92	100	88.9	87.5	krt, asm
10	96	100	100	87.5	skew, krt, ssq, sentr
Average	95.2	95	98.89	91.25	
SD	3.67	8.74	3.51	6.04	

asm = Angular second moment, con = contrast, corr = correlation, idm = inverse difference moment, krt = kurtosis, mv = mean value, sentr = sum of entropy, skew = skewness, ssq = sum of squares, svar = sum variance.

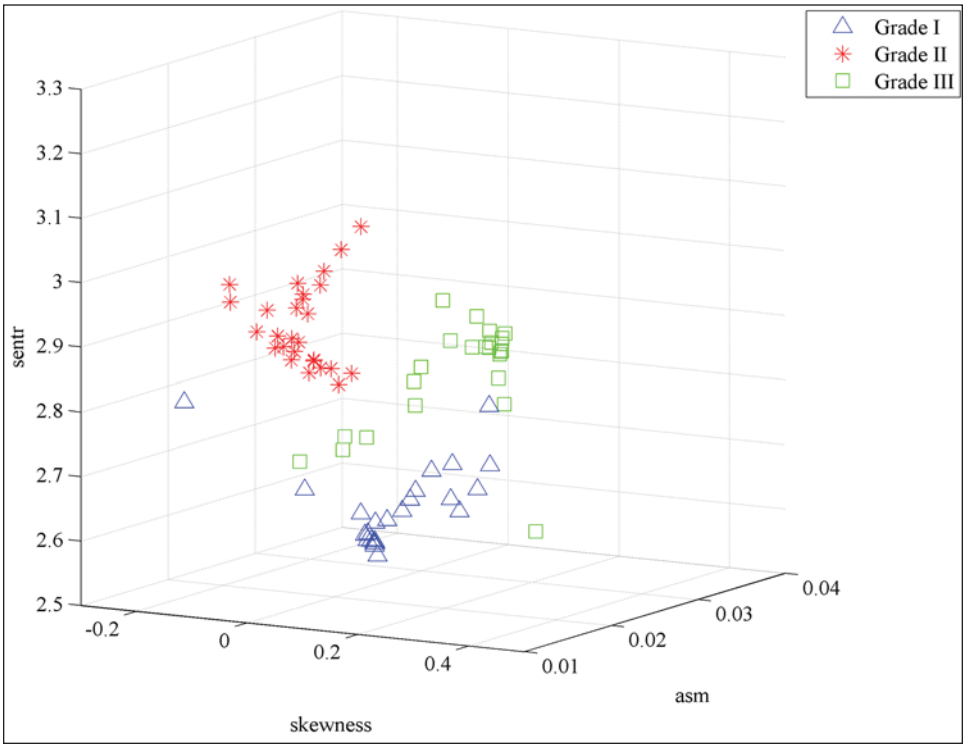

Figure 5 Scatter diagram of the 3 most frequently appearing features (skew, asm, sentr) at each repetition of the ECV.

First, it is possible to predict tumor grade using IHC-stained specimens; until now, breast tumor grading has been exclusively performed on H-E–stained specimens. Second, the texture of expressed ER nuclei strongly correlates with tumor grade; previously, only the ER status was used to investigate any such possible correlation. Thus we have seen through 3 different measurements that there is a meaningful correlation between ER status and tumor grade. The first uses the ER status estimated by the histopathologist, which has been already reported in literature,[5-9] the second utilizes a more objective estimation of ER status through a custom-developed computer-based method and the third exploits the texture of expressed ER nuclei. As far as we know, the second and third perspectives have not been previously reported in literature.

The PR system classified grade I tumors with 95% accuracy, grade II with 98.89% accuracy and grade III with 91.25% accuracy. It is interesting to examine how these results relate to ER status. The ER status averages of grade I, II and III tumors were ~77%, ~60% and ~39%, respectively. The respective variations for each malignancy group ranged from 65% to 90% for grade I, 40% to 80% for grade II and 0% to 78% for grade III. These data concern those cases that fall inside the box plots shown in Figure 4. It is possible that the significant variation in ER status that was observed in our data for grade III tumors was due to the existence of inherent tumor heterogeneity.[41-43] Another observation that reinforces this belief is that classification accuracy for grade III

Table IV *Comparative Results Illustrating the Overall Performance of the System Under Different Color Spaces, Using 2-D or 3-D Features and Different Classifiers*

Features	Color space	PNN (%)	Logistic regression (%)	SVM (%)	Nearest neighbor (%)
2D	Grayscale	93.0 ± 5.2	89.5 ± 7.4	92.8 + 6.2	93.2 ± 5.4
3D	RGB	92.8 ± 4.54	90.4 ± 5.4	93.2 ± 2.7	90.8 ± 4.6
	Lab	95.2 ± 3.67	92.4 ± 5.2	94.4 ± 2.8	93.6 ± 3.2

tumors was the lowest (91.25%) as compared with grade I (95%) and grade II (98.89%) tumors; higher grade tumors are usually composed of various cell populations of different grades, which can cancel out criteria that might be used to establish distinct boundaries for the separation of different grade tumors.[41-43] This may explain the reduced performance of the PR system for the recognition of grade III tumors. For grade I and II tumors, heterogeneity dominates to a lesser extent, allowing the PR system to be more precise and effective (with an accuracy of 98.89% and 95%, respectively).

It has to be stressed that the proposed system was validated using an external cross-validation process. The selection of the validation process is an important task; there are few validation processes that allow for the extraction of conclusions regarding the generalization of the methods used. Previous studies[26,27] have demonstrated that cross-validation samples should be kept external to the feature selection process. Moreover, in a previous study[26] researchers also assessed several techniques for estimating the generalization error. They showed that the external cross-validation error is among the most unbiased estimators of the generalization error. Hence, using the external cross-validation method enables us to argue that results (overall accuracy 95.2%) are indicative of the generalization ability of the system to new ER data. This adds an additional value to the results.

However, ECV cannot be used to propose a specific PR system's design with particular features. With this in mind, a possible way of designing a ready-to-use system for clinical trial could involve the selection of the most frequently appearing features that optimize the classification accuracy at each repetition of the ECV. In our study, such features were the skewness, angular second moment, and sum of entropy (Table II). Skewness describes the histogram's asymmetry and encodes intensity information. Angular second moment encodes the variations in ERs texture homogeneity. Finally, sum of entropy is a measure of texture randomness describing nuclei coarseness.

A by-product of this research is that it seems possible to perform grading directly on IHC-stained images containing positively expressed ER nuclei, with a relatively high accuracy of 95.2%. However, a tumor might not express any ER, though it resides at a specific malignancy level. Under such conditions, grading is only feasible on H-E–stained specimens. A very interesting extension of this study would be to investigate if the combination of textural information extracted on both IHC-stained and H-E–stained specimens might improve the grading of breast tumors.

Acknowledgments

We thank the Department of Pathology of the University Hospital of Patras for assisting with the peer evaluation of the H-E histologic specimens.

References

1. Parkin D, Bray F, Ferlay J, Pisani P: Estimating the world cancer burden: GLOBOCAN 2000. Int J Cancer 2001;94:153–156
2. Fitzgibbons PL, Page DL, Weaver D, Thor AD, Allred DC, Clark GM, Ruby SG, O'Malley F, Simpson JF, Connolly JL, Hayes DF, Edge SB, Lichter A, Schnitt SJ: Prognostic factors in breast cancer: College of American Pathologists Consensus Statement 1999. Arch Pathol Lab Med 2000;124:966–978
3. Stewart BW, Kleihues P (editors): World Cancer Report. Lyon, France, IARC Press, 2003, pp 2434–3439
4. Diaz LK, Sahin A, Sneige N: Interobserver agreement for estrogen receptor immunohistochemical analysis in breast cancer: A comparison of manual and computer-assisted scoring methods. Ann Diagn Pathol 2004;8:23–27
5. Desai SB, Moonim MT, Gill AK, Punia RS, Naresh KN, Chinoy RF: Hormone receptor status of breast cancer in India: A study of 798 tumours. Breast 2000;9:267–270
6. Zafrani B, Aubriot MH, Mouret E, De Crémoux P, De Rycke Y, Nicolas A, Boudou E, Vincent-Salomon A, Magdelénat H, Sastre-Garau X: High sensitivity and specificity of immunohistochemistry for the detection of hormone receptors in breast carcinoma: Comparison with biochemical determination in a prospective study of 793 cases. Histopathology 2000;37:536–545
7. Fuqua SAW, Schiff R, Parra I, Moore JT, Mohsin SK, Osborne CK, Clark GM, Allred DC: Estrogen receptor β protein in human breast cancer: Correlation with clinical tumor parameters. Cancer Res 2003;63:2434–2439
8. Vagunda V, Smardova J, Vagundova M, Jandakova E, Zaloudik J, Koukalova H: Correlations of breast carcinoma biomarkers and p53 tested by FASAY and immunohistochemistry. Pathol Res Pract 2003;199:795–801
9. Baqai T, Shousha S: Oestrogen receptor negativity as a marker for high-grade ductal carcinoma in situ of the breast. Histopathology 2003;42:440–447
10. Diaz LK, Sneige N: Estrogen receptor analysis for breast cancer: Current issues and keys to increasing testing accuracy. Adv Anat Pathol 2005;12:10–19
11. Kostopoulos S, Cavouras D, Daskalakis A, Kagadis GC, Kalatzis I, Georgiadis P, Ravazoula P, Nikiforidis G: Cascade pattern recognition structure for improving quantitative assessment of estrogen receptor status in breast tissue carcinomas. Anal Quant Cytol Histol 2008;30:218–225
12. Fowler AM, Solodin N, Preisler-Mashek MT, Zhang P, Lee AV, Alarid ET: Increases in estrogen receptor-α concentration in breast cancer cells promote serine 118/104/106-inde-

pendent AF-1 transactivation and growth in the absence of estrogen. FASEB J 2004;18:81–93

13. Shao W, Brown M: Advances in estrogen receptor biology: Prospects for improvements in targeted breast cancer therapy. Breast Cancer Res 2004;6:39–52
14. Zheng WQ, Lu J, Zheng JM, Hu FX, Ni CR: Variation of ER status between primary and metastatic breast cancer and relationship to p53 expression*. Steroids 2001;66:905–910
15. Raam S, Richardson GS, Bradley F, MacLaughlin D, Sun L, Frankel F, Cohen JL: Translocation of cytoplasmic estrogen receptors to the nucleus: Immunohistochemical demonstration utilizing rabbit antibodies to estrogen receptors of mammary carcinomas. Breast Cancer Res Treat 1983;3:179–199
16. Wolberg WH, Street WN: Computer-generated nuclear features compared with axillary lymph node status and tumor size as indicators of breast cancer survival. Hum Pathol 2002; 33:1086–1091
17. Wolberg WH, Street WN, Heisey DM, Mangasarian OL: Computer-derived nuclear "grade" and breast cancer prognosis. Anal Quant Cytol Histol 1995;17:257–264
18. Wolberg WH, Street WN, Mangasarian OL: Image analysis and machine learning applied to breast cancer diagnosis and prognosis. Anal Quant Cytol Histol 1995;17:77–87
19. Albert R, Müller JG, Kristen P, Harms H: Objective nuclear grading for node-negative breast cancer patients: Comparison of quasi-3D and 2D image-analysis based on light microscopic images. Lab Invest 1998;78:247–259
20. Tuczek HV, Fritz P, Schwarzmann P, Wu X, Mähner G: Breast carcinoma: Correlations between visual diagnostic criteria for histologic grading and features of image analysis. Anal Quant Cytol Histol 1996;18:481–493
21. Albert R, Müller JG, Kristen P, Schindewolf T, Kneitz S, Harms H: New method of nuclear grading of tissue sections by means of digital image analysis with prognostic significance for node-negative breast cancer patients. Cytometry 1996;24:140–150
22. Soong TT: Fundamentals of Probability and Statistics for Engineers. 22nd Edition. Chichester, West Sussex, England, Wiley, 2004, pp 34–38
23. Haralick R, Shanmugam K, Dinstein I: Textural features for image classification. IEEE Trans Syst Man Cybernetics 1973; 3:610–621
24. Mahmoud-Ghoneim D, Toussaint G, Constans JM, de Certaines JD: Three dimensional texture analysis in MRI: A preliminary evaluation in gliomas. Magn Reson Imaging 2003; 21:983–987
25. Palm C: Color texture classification by integrative co-occurrence matrices. Pattern Recognition 2004;37:965–976
26. Ambroise C, McLachlan GJ: Selection bias in gene extraction on the basis of microarray gene-expression data. Proc Natl Acad Sci USA 2002;99:6562–6566
27. Delogu P, Evelina Fantacci M, Kasae P, Retico A: Characterization of mammographic masses using a gradient-based segmentation algorithm and a neural classifier. Comput Biol Med 2007;37:1479–1491
28. Specht D: Probabilistic neural networks. Neural Networks 1980;3:109–118
29. Theodoridis S, Koutroumbas K: Pattern Recognition. Second edition. San Diego, Elsevier, 2003, pp 179–190
30. Burges C: A tutorial on support vector machines for pattern recognition. Data Mining and Knowledge Discovery 1998;2: 121–167
31. Veltri RW, Chaudhari M, Miller MC, Poole EC, O'Dowd GJ, Partin AW: Comparison of logistic regression and neural net modeling for prediction of prostate cancer pathologic stage. Clin Chem 2002;48:1828–1834
32. Pham NA, Morrison A, Schwock J, Aviel-Ronen S, Iakovlev V, Tsao MS, Ho J, Hedley DW: Quantitative image analysis of immunohistochemical stains using a CMYK color model. Diagn Pathol 2007;2:8
33. Cheng HD, Sun Y: A hierarchical approach to color image segmentation using homogeneity. IEEE Trans Image Process 2000;9:2071–2082
34. Chapman JA, Miller NA, Lickley HL, Qian J, Christens-Barry WA, Fu Y, Yuan Y, Axelrod DE: Ductal carcinoma in situ of the breast (DCIS) with heterogeneity of nuclear grade: Prognostic effects of quantitative nuclear assessment. BMC Cancer 2007;7:174
35. Selvarajan S, Wong KY, Khoo KS, Bay BH, Tan PH: Overexpression of c-erbB-2 correlates with nuclear morphometry and prognosis in breast carcinoma in Asian women. Pathology 2006;38:528–533
36. Daskalakis A, Kostopoulos S, Spyridonos P, Glotsos D, Ravazoula P, Kardari M, Kalatzis I, Davouras, Nikiforidis G: Design of a multi-classifier system for discriminating benign from malignant thyroid nodules using routinely H&E-stained cytological images. Comput Biol Med 2008;38:196–203
37. Kayser K, Radziszowski D, Bzdyl P, Sommer R, Kayser G: Towards an automated virtual slide screening: Theoretical considerations and practical experiences of automated tissue-based virtual diagnosis to be implemented in the Internet. Diagn Pathol 2006;1:10
38. Steinberg DM, Ali SZ: Application of virtual microscopy in clinical cytopathology. Diagn Cytopathol 2001;25:389–396
39. Kolles H, von Wangenheim A, Rahmel J, Niedermayer I, Feiden W: Data-driven approaches to decision making in automated tumor grading: An example of astrocytoma grading. Anal Quant Cytol Histol 1996;18:298–304
40. Belacel N, Boulassel M: Multicriteria fuzzy assignment method: A useful tool to assist medical diagnosis. Artificial Intelligence Med 2001;21:201–207
41. Latson L, Sebek B, Powell KA: Automated cell nuclear segmentation in color images of hematoxylin and eosin-stained breast biopsy. Anal Quant Cytol Histol 2003;25:321–331
42. Diekman C, He W, Prabhu N, Cramer H: Hybrid methods for automated diagnosis of breast tumors. Anal Quant Cytol Histol 2003;25:183–190
43. Harrison M, Coyne JD, Gorey T, Dervan PA: Comparison of cytomorphological and architectural heterogeneity in mammographically-detected ductal carcinoma in situ. Histopathology 1996;28:445–450